Plant Foods for Human Nutrition (2021) 76:219–225
https://doi.org/10.1007/s11130-021-00897-5

ORIGINAL PAPER

Synthesis of Resveratrol Loaded Hybrid Silica-PAMAM Dendrimer Nanoparticles With Emphases on Inducible Nitric Oxide Synthase and Cytotoxicity

Ceren Kececiler-Emir[1,2] · Esra Ilhan-Ayisigi[3,4] · Cigdem Celen-Erden[3] · Ayse Nalbantsoy[3] · Ozlem Yesil-Celiktas[3]

Received: 12 February 2021 / Accepted: 27 April 2021 / Published online: 5 May 2021

Abstract

Resveratrol is a naturally occurring polyphenolic compound exhibiting therapeutic activities. However, the stability can be altered by UV light, pH and changes in temperature. Encapsulation would be an ideal strategy to improve the stability and bioavailability. Thus, *trans*-resveratrol (Res) was encapsulated within hybrid nanoparticles consisted with silica and G4 polyamidoamine dendrimer (PAMAM) by sol-gel method. The diameters of synthesized nanoparticles (NPs) were at a range of 212–574 nm and the encapsulation efficiency was 86 %. RAW 264.7 murine macrophage cell line induced with endotoxin/lipopolysaccharide was treated with free resveratrol and Res-loaded NPs for assessing inhibition of inducible nitric oxide synthase (iNOS), where IC_{50} values of free resveratrol and Res-loaded NPs were 122.68 μM and 249.74 μM. As for cytotoxicity, IC_{50} values of free resveratrol were found as 176.57 μM and 201.54 μM for MCF-7 and MDA-MB-231 cells, whereas 197.16 μM and 219.07 μM for Res-loaded NPs for the respective cell lines. Overall, sol-gel technique proved to be an ideal technology as can be carried out under mild conditions and Res-loaded NPs have potential to be utilized in the industry.

Keywords Sol-gel · Nanoparticle · PAMAM · Resveratrol · Cytotoxicity · iNOS

Introduction

Resveratrol is a phytoalexin of the stilbene group synthesized from fruits under biotic or abiotic stress conditions, which has been utilized in the prevention of various diseases such as osteoarthritis [1], muscle atrophy in partial gravity [2], atherosclerosis [3] and cancer [4]. Resveratrol exhibits a powerful anti-carcinogenic effect, which leads to cell death of cancer cells through different pathways without cytotoxicity to healthy cells. Moreover, resveratrol and its derivatives are reported to be responsible for the alpha-mediated biological responses of different estrogen receptors observed in estrogen sensitive cancer cells [5], which makes it a suitable candidate for breast cancer. Indeed, recent research suggests that resveratrol reduces the proliferation of breast cancer cells [4] by acting as an antagonist to the estrogen receptor. For this reason, the activity of resveratrol differs from estrogen receptor positive (MCF-7) to estrogen receptor negative (MDA-MB-231) breast cancer cells [6]. However, resveratrol is susceptible to degradation and should be protected from UV light, temperature, pH changes, certain types of enzymes and moisture [7]. The encapsulation of pharmaceutical compounds is an ideal strategy to preserve the therapeutic efficiency, increase bioavailability and the dissolution rates [8]. Various techniques are applied, among them is sol-gel process utilized for encapsulation of particles at nanoscale based on a series of sequential chemical reactions and formation of a network via electrochemical interactions of the particles with surface charge. The advantages of the sol-gel process are purity, homogeneity and possibility to operate at low temperatures yielding controlled porosity [9]. Dendrimers, a core of

✉ Ozlem Yesil-Celiktas
ozlem.yesil.celiktas@ege.edu.tr

1 Bioengineering Department, Faculty of Chemical and Metallurgical Engineering, Yıldız Technical University, 34210 Istanbul, Turkey

2 Genetic and Bioengineering Department, Faculty of Rafet Kayis Engineering, Alanya Alaaddin Keykubat University, Antalya, Turkey

3 Department of Bioengineering, Faculty of Engineering, Ege University, 35100 Izmir, Turkey

4 Genetic and Bioengineering Department, Faculty of Engineering and Architecture, Ahi Evran University, Kirsehir, Turkey

polymeric drug delivery systems provide appropriate architectures for encapsulation of biological molecules and are comprised of branching, also known as surface groups and functional groups around the nucleus. Polyamidoamine (PAMAM) dendrimers are used as carrier in drug delivery systems to increase transepithelial permeability and to eliminate low bioavailability problems. Both amine-terminated dendrimers with cationic as well as carboxylic acid terminated anionic PAMAM modulate tight junctions in the gastrointestinal tract and thus are known to increase the transition between cells [10]. In this study, resveratrol is encapsulated by sol-gel technique using PAMAM. The most efficient form of tetraethylorthosilicate (TEOS) hydrolysate with PAMAM G-4 at different rates were formed and characterized. The cytotoxicity of resveratrol loaded silica-PAMAM nanoparticles (Res-loaded NPs) was examined in MCF-7 estrogen-dependent, estrogen-independent MDA-MB-231 breast cancer cells along with iNOS inhibitory activities.

Materials and Methods

Synthesis of Resveratrol-loaded Silica-PAMAM Nanoparticles by Sol-gel Synthesis

Resveratrol was encapsulated based on the method reported for sol-gel synthesis of silica-PAMAM dendrimer [11]. Briefly, TEOS was hydrolyzed by 0.1 M hydrochloric acid, corresponding to 0.25 M TEOS hydrolysate and mixed for 2.5 h at high speed. PAMAM G-4 dendrimer was diluted to 1.15 mM in 0.5 M Tris-HCl buffer (pH 7.6) before the mixing with TEOS hydrolysate and ethanolic resveratrol solution (7 mM) for 1 h. Various TEOS hydrolysate and PAMAM volumes *per* mL of reaction were tested to optimize the particle size. Subsequently, the reaction solution was centrifuged (MiniSpin®plus, Eppendorf, Hamburg, Germany) at 6000 *g* for 15 min, the particles were washed with distilled H_2O and lyophilized. The supernatant was separated from the nanoparticle pellet and quantified by UV-Vis spectrophotometer (Agilent, Santa Clara, USA) at 314 nm to determine the unloaded resveratrol. Calibration curves were established by dissolving 4 mg *trans*-resveratrol in 1 mL ethanol and diluted with PBS in the range 0.1–10 μg/mL. Encapsulation efficiency was expressed as the ratio of actual and theoretical loading. The analyses were carried out in duplicate.

Characterization and *In Vitro* Release Study

Size distributions were measured with Malvern Zetasizer Nano-ZS (Malvern Instruments Ltd, Worcestershire, UK). The results were determined by the average of three cycles of many scans. Fourier-Transform infrared spectra (FTIR) of empty-NPs, Res-loaded NPs and free resveratrol were determined by Perkin Elmer Spectrum Two instrument with an Attenuated Total Reflection (ATR) accessory between the wavelengths of 600–4000 cm^{-1}. For the morphological imaging, the lyophilized NPs were coated with gold and images were captured using scanning electron microscope (SEM) (Quanta 250 FEG). X-Ray diffraction (XRD) measurements of lyophilized NPs were carried out using X-ray diffractometer (Shimadzu, Japan) at a scanning rate of 4°/min in the 2θ range of 5 to 90°. The *in vitro* release experiments were performed by using the dialysis method with RES-loaded NPs in 10 mL of release medium (0.01 M PBS at intestinal pH 7.4 or 0.1 M HCl at gastric pH 1.2) under agitation at 37 °C. The dialysis bags agitated in HCl were introduced in another vessel containing 10 mL of PBS after 2 h. At predetermined time points, aliquots were taken out, and the release medium was replenished with the same volume of fresh medium. The amount of resveratrol released from the formulations was quantified by UV-Vis spectrophotometer (Agilent, Santa Clara, USA). Calibration curves of free resveratrol in PBS at pH 7.4 and HCl at pH 1.2 were performed, over the range 0.05–5 μg/mL ($R^2 > 0.999$) in both cases. The release curves were plotted based on the accumulative release percentage *versus* time.

Statistical Analysis

Statistical analyses were performed by Student's *t*-test. A probability value of $p \leq 0.05$ was considered to denote a statistically significant difference, and $p \leq 0.01$ was also used to show the power of the significance. IC_{50} values were determined within the range of ± 95 % confidence by GraphPad Prism (San Diego, CA).

Results and Discussion

Nanoparticle Synthesis, Characterization and *In Vitro* Release

Nanoparticle synthesis with sol-gel technique has several advantages like high purity, biocompatibility, thermal and chemical stability of the matrix, low processing temperature and easy control of the morphology [10]. In this study, hybrid nanoparticles were synthesized incorporating silica and PAMAM dendrimer. Various ratios of TEOS-PAMAM were investigated to observe the effects on particle sizes (Table 1). The decreasing concentration of TEOS resulted in a decrease in the particle diameter to a certain TEOS: PAMAM (50:100) ratio, whereas a marked increase was observed at TEOS:PAMAM ratio of 25:125. The inorganic precursor TEOS can affect the volume and diameter of particles and highly influence the diameter of particle pores [9]. Apart from size, polydispersity index (PDI) of nanoparticles are of prime

importance. These parameters are directly related to stability, biodistribution, and release of encapsulated compound. The values of PDI ranging from 0 to 0.5 are usually considered as monodisperse and homogenous, whereas higher values indicate polydispersity [12]. PDI values of nanoparticles at TEOS:PAMAM ratios of 75:75 and 100:50 were both 0.450 which can be interpreted as displaying a comparatively homogeneous particle size distribution. However, other samples with different ratios of TEOS:PAMAM have polydisperse characteristics. The mean hydrodynamic diameter of encapsulated resveratrol in colloidal mesoporous silica nanoparticles was reported as 283 nm with a PDI of 0.250 after drug loading [13]. The results obtained by various ratios of TEOS:PAMAM indicated that the particle diameter was effective only up to a certain point. As the average diameter of nanoparticles prepared at a ratio of 100:50 was 279 nm with the lowest PDI value, nanoparticles synthesized under this condition was further analyzed for encapsulation efficiency, morphology, cytotoxicity and iNOS activity. For resveratrol-loaded NPs, the mean particle size was 340 nm (Fig. 1a). The outer topographies of empty and Res-loaded NPs were explored using SEM. From the micrographs, it is clearly seen that empty and Res-loaded NPs exhibited spherical structure and smooth surfaces (Fig. 1b and c). Sciortino et al [14] have reported the synthesis of nanoparticles using TEOS, where morphology of particles were slightly different from the SEM images presented in this study. The differences can be attributed to varying TEOS ratios during synthesis. As for encapsulation, 75 % ±7 efficiency was achieved owing to the branching of PAMAM dendrimer. The particle sizes of liposome-loaded Ca-alginate microspheres for controlled release of resveratrol were determined to be much larger, ranging between 387 and 440 μm with an encapsulation efficiency of 85 % [15]. Smaller particle sizes with similar encapsulation efficiencies might be favorable for release of resveratrol due to larger surface areas. Res-loaded-NPs, free resveratrol, and empty NPs were characterized by ATR-FTIR spectroscopy as well (Fig. 1d). The peaks centered at 800 and 970 cm^{-1} of both of empty NPs and Res-loaded NPs can be associated with the stretching frequencies, whereas the peak at 1646 cm^{-1} can be assigned to the C = O stretching vibration inside the PAMAM dendrimer which is also in good agreement with our previous study [11]. Moreover, the band observed in both samples at around 1060–1070 cm^{-1} can be assigned to the stretching modes of the siloxane framework, ≡Si − O–Si≡ [16]. The free resveratrol displayed characteristic absorption bands at 3240 cm^{-1} for O − H stretching because of the alcoholic group, 965 cm^{-1} for trans-olefinic bond, 1586 cm^{-1} for C = C stretching of the aromatic ring, 1147 cm^{-1} for C–O stretching, respectively. Although Res-loaded NPs performed all characteristic absorption peaks of empty NPs, the characteristic peak of resveratrol in Res-loaded NPs was not apparent, indicating that the compound was encapsulated in the core of loaded NPs successfully. The content of resveratrol was too negligible to be detected when compared with the content of silica-PAMAM, which is in agreement with the study of resveratrol encapsulation into poly(D, L-lactide-co glycolide acid) nanoparticles [17]. The FTIR results also proved that there was no potential chemical reaction between resveratrol and any other formulation ingredients. These results corroborate the XRD data, which is a widely technique used to investigate the crystalline nature of the matter. The diffraction spectra of empty NPs demonstrated a broad and diffused band depicting the amorphous nature of silica-PAMAM NPs. On the other hand, the XRD pattern of Res-loaded NPs showed some unique diffraction peaks of resveratrol present in the nanoparticles in addition to the broad peak of silica-PAMAM NPs, suggesting that the resveratrol have not been completely converted to its amorphous form in the nanoparticle matrices and have a local crystal arrangement, as confirmed by specific resveratrol diffraction peaks at 16.3, 19.2, 22.3, 28.3 and 45.4º [18] (Fig. 1e). Therefore, the local presentation of resveratrol in the crystalline form may affect the release from the NP matrices and result in the slower release as compared to a system where the drug is present in an amorphous state [19]. The *in vitro* release profile of resveratrol from Res-loaded NPs is presented as a cumulative release at pH 1.2 and 7.4, representing stomach and intestine (Fig. 1f). At both pH values, Res-loaded NPs exhibited a slow-release profile, which could be attributed to the presentation of resveratrol in crystalline form, where the cumulative releases were less than 25 % within 2 h. At pH 7.4, resveratrol was released up to 54 % in the first 5 h followed by 63 % in 24 h. However, Res-loaded NPs transferred from gastric pH of 1.2, mimicking stomach content to the intestine, showed 28 % release in the first 5 h followed by up to only 37 % release over 24 h. After 48 h, the total cumulative Res release from both dissolution media of pH 7.4 continuously and pH 7.4 which transferred from gastric pH of 1.2 reached 69 and 47 %, respectively. The overall release behavior could be attributed to the kinetic solubility of resveratrol, which is affected by dissolution media. Resveratrol is reported to remain un-ionized under acidic conditions and poorly water soluble [20]. Presumably, the pH level of the microenvironment of nanoparticles decreased partially due to the acidic residues from the previous stomach type dissolution medium, causing delay of resveratrol release in 48 h period. Previously, PO_3- or NH_2- functionalized mesoporous silica nanoparticles showed 40 % of total release in 24 h at pH 5.5, whereas equal or more than 65 % release occurred at pH 7.4 during the 24 h period [21]. Furthermore, the cumulative resveratrol release percentages of Res-loaded poly(lactic-co-glycolic acid) (PLGA) NPs and Res-loaded-galactosylated PLGA NPs were reported to be less than 43 % in water within 8 h [22]. The *in vitro* release data suggests that the slow-release allows the majority of resveratrol to be retained in NPs when transporting through the gastrointestinal tract, which is favorable for absorption via NPs. The oral bioavailability of resveratrol is very low (< 1 %) due to rapid and extensive metabolism and formation of various metabolites such as resveratrol glucuronides and sulfates [23]. The prolonged detection of low plasma levels of these resveratrol metabolites

after oral consumption suggests that resveratrol is partly metabolized in the small intestine and then distributed to various tissues mainly in its conjugated forms and enteric recirculation of these conjugated metabolites are reabsorbed after intestinal hydrolysis [24]. Thus, the authors concluded that delayed and noncompleted release of resveratrol from Res-loaded NPs transferred from gastric pH of 1.2 to 7.4 might enhance its bioavailability of the released resveratrol due to controlled intestinal hydrolysis.

Cytotoxic and iNOS Activities of Synthesized Nanoparticles

The cellular responses of estrogen dependent MCF-7 cancer cells and estrogen-independent MDA-MB-231 cells might differ when supplemented with natural compounds and drug molecules. Thus, both cancer cells were treated with resveratrol, Res-loaded and empty nanoparticles at three different concentrations (50, 5, 0.50 μg/mL) (Fig. 2a and b). According to the MTT assay, cell viabilities of resveratrol were 17.09 ± 0.40 and 37.60 ± 0.52 % for MCF-7 and MDA-MB-231 cells at 50 μg/mL, whereas Res-loaded NPs exhibited viabilities of 26.45 ± 0.10 and 34.13 ± 0.61 % for the respected cells. Biocompatibility of empty nanoparticles is of prime importance [25] in order to associate the cytotoxic effect with the drug or the molecule of interest. Thus, it is worth to mention that empty nanoparticles were not toxic to the cells as 94.35 ± 0.94 and 90.86 ± 2.46 % of cell viabilities were retained of estrogen dependent and independent cells. However, 5 and 0.5 μg/mL concentrations of resveratrol and Res-loaded NPs have not exerted significant cytotoxicity against both cell lines. IC_{50} values of Res-loaded NPs were determined as 197.16 and 219.07 μM for MCF-7 and MDA-MB-231 cells, whereas 176.57 and 201.54 μM for resveratrol, respectively. The slight differences in IC_{50} values of Res-loaded NPs and free resveratrol indicate the coherency between the rate of release and cellular uptake, which proves the adequacy of silica-PAMAM dendrimer structure formulated. Resveratrol was reported to inhibit cell proliferation and viability in both cell lines. For instance, with respect to MDA-MB-231, resveratrol with a concentration of up to 200 μM lowered the expression and inhibited ribonucleotide reductase activity [6]. On the other hand, increasing resveratrol concentration was noted to decrease proliferation of MCF-7 by blocking the cancer cell cycle [26]. Moreover, key tumor-suppressive miRNAs were found to be modulated by resveratrol proving to have a key role in breast cancer cell death [27]. In another study, resveratrol doped monodisperse silica particles prepared with poloxamer 188 by high pressure homogenization exhibited a particle size of 198.6 nm and effectively inhibited HepG2 cells [28]. Another aspect to evaluate the efficacy of resveratrol and encapsulated form was to assess nitric oxide (NO) (Fig. 2c) acting as a regulatory and pro-inflammatory mediator. Thus, the inhibition of iNOS was examined after 24 h of the application of Res-loaded NPs and free resveratrol to the RAW-264.7 cells induced by lipopolysaccharide (LPS), a component of cellular walls of gram-negative bacteria. IC_{50} values were determined as 0.249 and 0.127 μM, respectively. It is well known that one of the hallmarks of inflammation is the activation of iNOS, an intracellular enzyme responsible for oxidation of L-arginine to the reactive gaseous free radical NO [29]. Overexpression of iNOS has been noted in cases of breast cancer and other cancer types [30]. For instance, 10 μg/mL of resveratrol showed anticancer effects by raising iNOS expressions in HepG2 human liver cancer cells [31]. In another study, resveratrol not only attenuated the expression of iNOS and NO production, but also reduced COX-2 expression and PGE2 production in A549 cells treated with carbon black nanoparticles, which act as the core component of many ultrafine pollutants [32]. For intervention of hepatocellular carcinoma, resveratrol elevated the protein and mRNA expression of hepatic nuclear factor E2-related factor 2, providing evidence that inflammatory response mediated by this factor might be suppressed [26]. Additionally, resveratrol was mentioned to exert a toxic effect against tumor-induced macrophages but noted to reduce by toll-like receptor activation as a result of stimulation by LPS [33]. Although, amorphous silica nanoparticles without any drug constituent were reported to generate reactive oxygen species in cultured RAW264.7 cells, which triggered pro-inflammatory responses both *in vivo* and *in vitro* [34], Res-loaded silica-PAMAM nanoparticles inhibited iNOS with an IC_{50} value of 0.249 μM based on our findings. Indeed, an anti-inflammatory drug conjugated to hydroxyl terminated generation-4 PAMAM dendrimer significantly attenuated inflammation by suppressing pro-inflammatory cytokines such as TNF-α, IL-1β, CCL-3, IL-6 and reduced iNOS in LPS activated RAW 264.7 by inhibiting NF-κB activation and its nuclear translocation significantly more as compared to the free drug [35]. Consequently, supplementation of resveratrol and encapsulated forms inhibiting NO synthesis by iNOS might be interpreted as a potential therapeutic remedy for inflammatory diseases or means of protection against inflammation.

Table 1 The effects of different TEOS:PAMAM ratios on mean particle size (volumes are given for *per* milliliter synthesis reaction)

Samples	TEOS (μL)	PAMAM (μL)	Average diameter (nm)
1	125	25	488
2	100	50	279
3	75	75	352
4	50	100	212
5	25	125	574
6 (drug loaded)	100	50	340

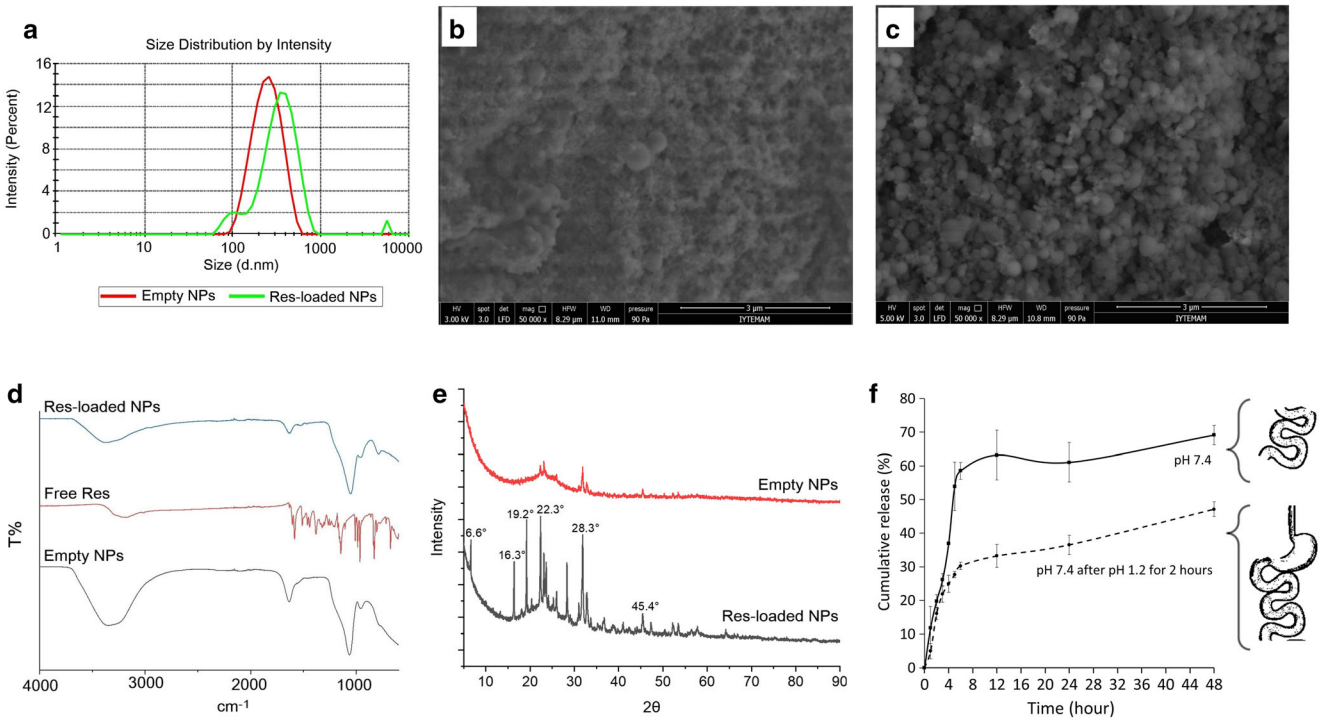

Fig. 1 Characterizations of hybrid nanoparticles synthesized. Size distributions of empty and Res-loaded NPs (**a**), SEM images of empty (**b**) and Res-loaded NPs (**c**), FTIR spectra of Res-loaded and empty NPs along with free resveratrol (**d**), XRD patterns of Res-loaded and empty NPs (**e**), resveratrol release profile from NPs at pH 7.4 mimicking intestine (top) and pH 7.4 followed by pH 1.2 for 2 h mimicking stomach and intestine (bottom) (**f**)

Conclusions

This study was aimed to develop a nanoencapsulation method to enclose resveratrol as a cargo into a hybrid matrix formed by silica and PAMAM. Res-loaded NPs exhibited a mean particle size of 340 nm, whereas the encapsulation efficiency was 86 %, owing to the branched repeating units of PAMAM G4 dendrimer. The Res-loaded NPs inhibited iNOS with an IC_{50} value of 249.74 μM and proved to be effective against estrogen positive and negative breast cancer cells with IC_{50} values of 197.16 and 219.07 μM, respectively. As this study has shown, combining dendrimers with silica through sol-gel synthesis is an ideal approach for protecting the cargo from degradation and allowing controlled release.

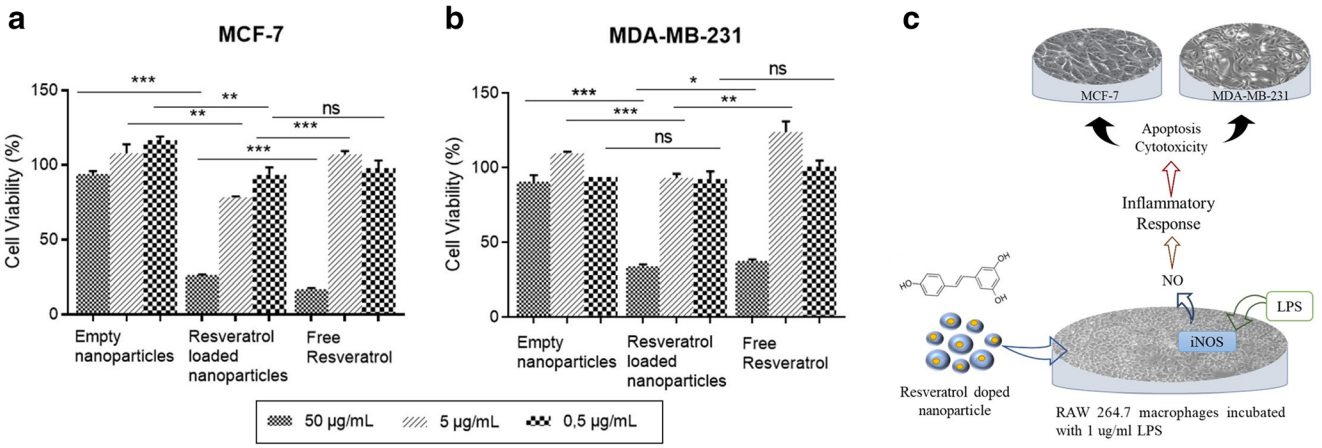

Fig. 2 Cell viability results of free resveratrol, Res-loaded and empty NPs in MCF-7 (**a**) and MDA-MB-231 cells after 48 h (**b**). The asterisk (*) indicates the significant difference with the control group for one-way ANOVA and Student's *t*-test (*$p < 0.05$ Res-loaded vs. empty NPs as control or free resveratrol alone). The experiments were performed in triplicates. Plots are mean ± S.E.M. ($n = 3$), depiction of the effect of Res-loaded NPs on LPS induced RAW-264.7 macrophages and iNOS inhibition (**c**)

Supplementary Information The online version contains supplementary material available at https://doi.org/10.1007/s11130-021-00897-5.

Acknowledgements This work was supported by TUBITAK 2209-A research project grant (1919B011400901).

Declarations

Conflict of Interest The authors declare no conflict of interest.

References

1. Zhang G, Zhang H, You W et al (2020) Therapeutic effect of resveratrol in the treatment of osteoarthritis via the MALAT1/miR-9/NF- B signaling pathway. Exp Ther Med 19:2343–2352
2. Mortreux M, Riveros D, Bouxsein ML, Rutkove SB (2019) A moderate daily dose of resveratrol mitigates muscle deconditioning in a Martian gravity analog. Front Physiol 10:899
3. Hong M, Li J, Li S, Almutairi MM (2020) Resveratrol derivative, *trans*-3, 5, 4'-trimethoxystilbene, prevents the developing of atherosclerotic lesions and attenuates cholesterol accumulation in macrophage foam cells. Mol Nutr Food Res 64:e1901115
4. Sinha D, Sarkar N, Biswas J, Bishayee A (2016) Resveratrol for breast cancer prevention and therapy: preclinical evidence and molecular mechanisms. Semin Cancer Biol 40–41:209–232
5. Han Y, Jo H, Cho JH et al (2019) Resveratrol as a tumor-suppressive nutraceutical modulating tumor microenvironment and malignant behaviors of cancer. Int J Mol Sci 20:925
6. Pozo-Guisado E, Alvarez-Barrientos A, Mulero-Navarro S et al (2002) The antiproliferative activity of resveratrol results in apoptosis in MCF-7 but not in MDA-MB-231 human breast cancer cells: cell-specific alteration of the cell cycle. Biochem Pharmacol 64:1375–1386
7. Zupančič Š, Lavrič Z, Kristl J (2015) Stability and solubility of trans-resveratrol are strongly influenced by pH and temperature. Eur J Pharm Biopharm 93:196–204
8. Yesil-Celiktas O, Cetin-Uyanikgil EO (2012) *In vitro* release kinetics of polycaprolactone encapsulated plant extract fabricated by supercritical antisolvent process and solvent evaporation method. J Supercrit Fluids 62:219–225
9. Ilhan-Ayisigi E, Yesil-Celiktas O (2018) Silica-based organic-inorganic hybrid nanoparticles and nanoconjugates for improved anticancer drug delivery. Eng Life Sci 18:882–892. https://doi.org/10.1002/elsc.201800038
10. Yulizar Y, Juliyanto S, Sudirman et al (2021) Novel sol-gel synthesis of CeO2 nanoparticles using *Morinda citrifolia* L. fruit extracts: structural and optical analysis. J Mol Struct 1231:129904
11. Yesil-Celiktas O, Pala C, Cetin-Uyanikgil EO, Sevimli-Gur C (2017) Synthesis of silica-PAMAM dendrimer nanoparticles as promising carriers in neuro blastoma cells. Anal Biochem 519:1–7. https://doi.org/10.1016/j.ab.2016.12.004
12. Yesil-Celiktas O, Cumana S, Smirnova I (2013) Silica-based monoliths for enzyme catalyzed reactions in microfluidic systems with an emphasis on glucose 6-phosphate dehydrogenase and cellulase. Chem Eng J 234:166–172
13. Summerlin N, Qu Z, Pujara N et al (2016) Colloidal mesoporous silica nanoparticles enhance the biological activity of resveratrol. Colloids Surf B Biointerfaces 144:1–7
14. Sciortino M, Alonzo G, Ciriminna R, Pagliaro M (2011) Sol-gel microcapsulation in silica-based particles: a comparative study. Silicon 3:77–83
15. Balanč B, Trifković K, Đorđević V et al (2016) Novel resveratrol delivery systems based on alginate-sucrose and alginate-chitosan microbeads containing liposomes. Food Hydrocoll 61:832–842
16. Wencel D, Dolan C, Barczak M et al (2013) Synthesis, tailoring and characterization of silica nanoparticles containing a highly stable ruthenium complex. Nanotechnology 24:365705. https://doi.org/10.1088/0957-4484/24/36/365705
17. Wan S, Zhang L, Quan Y, Wei K (2018) Resveratrol-loaded PLGA nanoparticles: enhanced stability, solubility and bioactivity of resveratrol for non-alcoholic fatty liver disease therapy. R Soc Open Sci 5:181457. https://doi.org/10.1098/rsos.181457
18. Vankayala JS, Battula SN, Kandasamy R et al (2018) Surfactants and fatty alcohol based novel nanovesicles for resveratrol: process optimization, characterization and evaluation of functional properties in RAW 264.7 macrophage cells. J Mol Liq 261:387–396. https://doi.org/10.1016/j.molliq.2018.04.058
19. Saralkar P, Dash AK (2017) Alginate nanoparticles containing curcumin and resveratrol: preparation, characterization, and *in vitro* evaluation against DU145 prostate cancer cell line. AAPS PharmSciTech 18:2814–2823. https://doi.org/10.1208/s12249-017-0772-7
20. Pentek T, Newenhouse E, O'Brien B, Singh Chauhan A (2017) Development of a topical resveratrol formulation for commercial applications using dendrimer nanotechnology. Molecules 22:137. https://doi.org/10.3390/molecules22010137
21. Chaudhary Z, Subramaniam S, Khan GM et al (2019) Encapsulation and controlled release of resveratrol within functionalized mesoporous silica nanoparticles for prostate cancer therapy. Front Bioeng Biotechnol 7:225. https://doi.org/10.3389/fbioe.2019.00225
22. Siu FYK, Ye S, Lin H, Li S (2018) Galactosylated PLGA nanoparticles for the oral delivery of resveratrol: enhanced bioavailability and *in vitro* anti-inflammatory activity. Int J Nanomed 13:4133–4144. https://doi.org/10.2147/IJN.S164235
23. Sergides C, Chirilă M, Silvestro L et al (2016) Bioavailability and safety study of resveratrol 500 mg tablets in healthy male and female volunteers. Exp Ther Med 11:164–170. https://doi.org/10.3892/etm.2015.2895
24. Wenzel E, Somoza V (2005) Metabolism and bioavailability of *trans*-resveratrol. Mol Nutr Food Res 49:472–481. https://doi.org/10.1002/mnfr.200500010
25. Vaitkuviene A, Ratautaite V, Mikoliunaite L et al (2014) Some biocompatibility aspects of conducting polymer polypyrrole evaluated with bone marrow-derived stem cells. Colloids Surf A Physicochem Eng Asp 442:152–156. https://doi.org/10.1016/j.colsurfa.2013.06.030
26. Bishayee A, Barnes KF, Bhatia D et al (2010) Resveratrol suppresses oxidative stress and inflammatory response in diethylnitrosamine-initiated rat hepatocarcinogenesis. Cancer Prev Res 3:753–763
27. Venkatadri R, Muni T, Iyer AKV et al (2016) Role of apoptosis-related miRNAs in resveratrol-induced breast cancer cell death. Cell Death Dis 7:e2104
28. Meng XP, Wang YF, Wang ZP (2016) Anti-hepatocarcinoma effects of resveratrol loaded solid nanodispersion by a new material nano silica. In: Proceedings of the 2016 6th International Conference on Applied Science, Engineering and Technology. pp 297–302
29. Wang GJ, Chen YM, Wang TM et al (2008) Flavonoids with iNOS inhibitory activity from *Pogonatherum crinitum*. J Ethnopharmacol 118:71–78. https://doi.org/10.1016/j.jep.2008.03.005
30. Granados-Principal S, Liu Y, Guevara ML et al (2015) Inhibition of iNOS as a novel effective targeted therapy against triple-negative breast cancer. Breast Cancer Res 17:25. https://doi.org/10.1186/s13058-015-0527-x

31. Jiang Q, Yang M, Qu Z et al (2017) Resveratrol enhances anticancer effects of paclitaxel in HepG2 human liver cancer cells. BMC Complement Altern Med 17:477
32. Hsu HT, Tseng YT, Wong WJ et al (2018) Resveratrol prevents nanoparticles-induced inflammation and oxidative stress via down-regulation of PKC-α and NADPH oxidase in lung epithelial A549 cells. BMC Complement Altern Med 18:211
33. Achy-Brou CAA, Billack B (2016) Lipopolysaccharide attenuates the cytotoxicity of resveratrol in transformed mouse macrophages. Plant Foods Hum Nutr 71:272–276
34. Park EJ, Park K (2009) Oxidative stress and pro-inflammatory responses induced by silica nanoparticles *in vivo* and *in vitro*. Toxicol Lett 184:18–25
35. Sharma R, Kambhampati SP, Zhang Z et al (2020) Dendrimer mediated targeted delivery of sinomenine for the treatment of acute neuroinflammation in traumatic brain injury. J Control Release 323: 361–375